

# Study on inherent neutron sources in MSR

Rui-Min Ji<sup>1,2</sup> · Cheng-Gang Yu<sup>1</sup> · Ming-Hai Li<sup>1</sup> · Rui Yan<sup>1</sup> · Yang Zou<sup>1</sup> · Gui-Min Liu<sup>1</sup>

Received: 9 January 2017 / Revised: 26 February 2017 / Accepted: 2 March 2017 / Published online: 13 March 2018  
© Shanghai Institute of Applied Physics, Chinese Academy of Sciences, Chinese Nuclear Society, Science Press China and Springer Nature Singapore Pte Ltd. 2018

**Abstract** The molten salt reactor (MSR) has received much recent attention. The presence of beryllium and the mixing of actinides with light nuclei in the fuel salt result in a relatively strong neutron source that can affect the surveillance at subcritical and transient characteristics during operation. In this study, we predict the inherent neutron sources based on a MSR model. The calculation shows that in the fresh core, the inherent neutron sources are mainly from alpha-induced neutrons. After power operation, the inherent neutron sources become remarkably stronger due to photoneutrons. Although being an insignificant part in the total neutron population during operation, the inherent neutron sources can be used as the installed neutron source after shutdown. If the MSR has continuously operated at full power (2 MWt) for 10 days, then there would be no need for the installed source within 80 days after shutdown. After operating constantly for 500 days, the installed neutron source can be eliminated within 2 years after shutdown.

**Keywords** MSR · Fuel salt · Inherent neutron source · Photoneutron · Alpha-induced neutron

---

This work was supported by the Chinese TMSR Strategic Pioneer Science and Technology Project under Grant No. XDA02010000.

✉ Yang Zou  
zouyang@sinap.ac.cn

✉ Gui-Min Liu  
liuguimin@sinap.ac.cn

<sup>1</sup> Shanghai Institute of Applied Physics, Chinese Academy of Sciences, Jiading Campus, Shanghai 201800, China

<sup>2</sup> University of Chinese Academy of Sciences, Beijing 100049, China

## 1 Introduction

Neutrons produced by reactions other than neutron-induced fission are called neutron sources. Neutron sources in the reactor are crucial to the surveillance of unexpected criticality events under the condition of startup or shutdown [1]. By supporting the fission rate in the subcritical reactor at sufficiently high levels, neutron sources make the surveillance highly reliable. Neutron sources can be classified as either an inherent or installed neutron source. The inherent neutron sources, mainly referred to photoneutrons, alpha-induced neutrons, and spontaneous fission neutrons produced in the core, are related to burn-up history. Generally, the inherent neutron sources in the fresh core are rather weak. Therefore, primary sources such as <sup>252</sup>Cf and <sup>241</sup>Am-Be sources are installed and used for the startup of a fresh reactor. However, the constituent isotopes of primary sources are transmuted by the neutron capture in the operating reactor. This reduces the lifespan of the primary sources. Thus, secondary sources are installed together with primary sources and begin to produce neutrons only after activation in the reactor. If the inherent source terms are sufficiently strong enough after operation, then secondary neutron sources would not be required [2, 3]. Besides, secondary neutron sources may be broken after commissioning for years according to Qinshan Nuclear Power Plant (NPP) [4]. In recent years, Chinese NPPs like Daya Bay NPP [4] and Changjiang NPP [5] have analyzed using spent fuel assemblies instead of secondary neutron sources in the refueling process.

In the molten salt reactors (MSRs), a mixture of actinides and light nucleus like beryllium, lithium, and fluorine is used as the fuel and the coolant at the same time. Therefore, there is a strong alpha-induced neutron source

even in the fresh core. Because of the beryllium in the fuel, the photoneutrons are built up by power operation. Accordingly, the inherent neutron sources can play the role of installed sources when the reactor is shutdown. Such experience has been gained on the VVR-M reactor [6] and the miniature neutron source reactors (MNSR hereafter) [7, 8]. The VVR-M reactor had power that was increased fivefold from 2 to 10 MW. It has been operating at the St. Petersburg Institute of Nuclear Physics since 1959. The MNSRs have been operating in Syria, Ghana, and China since the 1990s. Both in the VVR-M and MNSR, the metallic beryllium reflector is the secondary neutron source. The molten salt reactor experiment (known simply as MSRE) was designed, built, and operated by Oak Ridge National Laboratory (ORNL) during the 1960s according to technical reports [9].

In the reports of MSRE, the inherent neutron sources were calculated by ORNL staff using analytical methods and cross-sectional data available in the early 1960s. Their results show that inherent neutron sources in MSRE with the fresh fuel [10–12] were primarily from  $(\alpha, n)$  reactions and the strength was determined by the compositions of the fuel salt. In their calculation, the photoneutron source was underestimated because the probability of one photon producing a photoneutron was approximated by the ratio of the  ${}^9\text{Be}(\gamma, n)$  cross section to the total cross section for photons interactions in the fuel mixture. The  ${}^9\text{Be}(\gamma, n)$  microscopic cross section of 0.5 mb was used, while the total cross section was evaluated to be 2 MeV. The inherent neutron sources of the MSRE were recalculated in recent years [13]. Calculations were made using a representative spherical reactor. The fuel salt depletion was simulated using ORIGEN. The inherent neutron sources generated by  $(\alpha, n)$  reactions and spontaneous fission were calculated using SOURCES4C [14], and the  $(\alpha, n)$  reaction rate was calculated with the updated  ${}^9\text{Be}(\gamma, n)$  cross sections and the gamma spectrum at a given energy fission of  ${}^{235}\text{U}$ . The recalculated reaction rates were markedly greater than the original ones. However, the gamma absorption and leakage in the core were ignored. The photoneutron production rate may be overestimated for fuel with high Z elements like zirconium.

The objective of this work is to calculate the strength of the inherent neutrons as a function of the operation and cooling time based on the MSR model.

## 2 MSR configurations

A 2 MWt experimental molten salt reactor aiming at the thorium-cycle research was designed by thorium molten salt reactor (TMSR) Group of Chinese Academy of Sciences (CAS) [15, 16]. This work used a full whole

simplified model. The initial fuel is  ${}^7\text{LiF}\text{-BeF}_2\text{-ThF}_4\text{-UF}_4$  (68–29–0.24–2.76 mol%) with 99.95% abundance of  ${}^7\text{Li}$  and 16.20% enrichment of  ${}^{235}\text{U}$ . The initial inventory of  ${}^{235}\text{U}$  is 32.82 kg, and the fuel volume in the core is  $0.54\text{ m}^3$ . The fuel flows from the lower head up through channeled regions in the graphite lattices and into the upper head. The nominal inlet temperature and outlet temperature of the fuel salts are 600 and 620 °C, respectively. The geometry parameters are listed in Table 1. MSR schematics are shown in Fig. 1. The reactor includes a central zone, an active zone, a reflector zone, the up and down salt chambers, and the vessel. In the central zone there is one channel used for irradiation surrounded by the salt, which is presented as part A in Fig. 1. In the active zone, the neatly arranged graphite blocks host the circulating salt, which is presented as part B in Fig. 1. In the reflector zone, the graphite blocks host the control rods, detectors, etc. The vessel and tubes used in the central channel to protect irradiation samples from fuel salts are made up of Hastelloy-N alloy.

## 3 Methodology

### 3.1 Production mechanisms of the inherent neutron sources

#### 3.1.1 Photoneutrons

The photoneutron production occurs due to absorption of photons by reactor materials above specific energy thresholds. In spite of low cross sections of  $(\gamma, n)$  reactions, the abundance of high-energy photons and the large number of targets such as beryllium and deuterium would generate a large amount of photoneutrons. In addition, photoneutrons are important during the design and operation of reactors because their behaviors are similar to the delayed neutrons [6, 7]. Considering the  ${}^{235}\text{U}$  fission in the infinite beryllium medium, the fraction of the delayed photoneutrons is  $15 \times 10^{-5}$ , and the average lifetime is 3.33 h. This is much longer than the delayed fission neutron (12.74 s). A discussion on the photons and the target nuclides is presented as follows.

In the fresh core, photons are mainly from the decay of uranium and thorium isotopes [9]. After power operation, many more photons are produced when the fuel undergoes fission as well as in the process of neutron capture by the fuel, structural materials, and other elements. The photons can be divided into prompt and delayed ones. The prompt photons are generated within  $10^{-11}$  s after the fission event. The photons are considered to be delayed if they are emitted long after the fission event such as the high-energy

**Table 1** MSR characteristic parameters

Region	Dimension	Values (cm)
Central zone	Size of this zone	5.1
	Inner diameter of the channel	3.8
	Thickness of the Hastelloy-N tube	0.1
Active zone	Height	110
	Outer diameter	110
	Size of the lattice	5.1
Reflector zone	Thickness of top, bottom and side reflector	40
	Diameter of channels	6
	Distance between the channels and the active zone	9
Vessel	Thickness	2
Reactor	Outer diameter	195
	Height	251

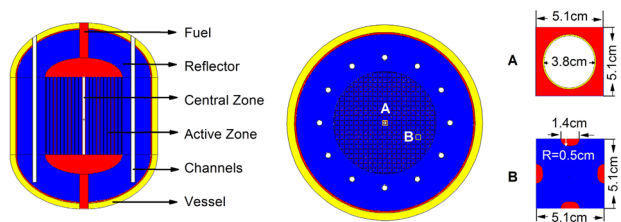


**Fig. 1** (Color online) The side view (left) and the top view (right) of the MSR (red: fuel salt; blue: graphite; yellow: Hastelloy-N alloy; white: control rods channel and types of detector channels surround the active region)

photons emitted by long-life fission products like  $^{140}\text{La}$ ,  $^{132}\text{Se}$ ,  $^{131}\text{Te}$ ,  $^{87}\text{Kr}$ ,  $^{88}\text{Kr}$ .

In our design, there are four nuclides that can produce photoneutrons in the fresh fuel. The cross sections are shown in Fig. 2 (left). The threshold energy of the  $^9\text{Be}(\gamma, n)$  reaction is about 1.67 MeV, and the cross section is lower than 1 mb in general within the region of interest. Except for beryllium, the  $(\gamma, n)$  reaction threshold energies of other nuclides are noticeably greater than 5 MeV, yet their cross sections are one order of magnitude larger than  $^9\text{Be}(\gamma, n)$  at high-energy region. Therefore, all targets with large quantities in the fuel may make a great contribution

to the photoneutron yields. However, there are few photons over 5 MeV shortly after the shutdown. Consequently, the photoneutrons originate from the  $^9\text{Be}(\gamma, n)$  reaction after the shutdown.

### 3.1.2 Alpha-induced neutron

Neutron production from the  $(\alpha, n)$  reactions takes place when the energetic alpha particles meet various light nuclides such as  $^7\text{Li}$ ,  $^9\text{Be}$ , and  $^{19}\text{F}$  in the fuel. The  $(\alpha, n)$  cross sections of  $^7\text{Li}$ ,  $^9\text{Be}$  and  $^{19}\text{F}$  are shown in Fig. 2 (right). The threshold energies vary widely depending upon the target nuclides, and all of them are lower than 4.5 MeV. In the reactor, alpha particles are mainly emitted by actinides and their energies are mostly lower than 10 MeV [10], which means the reactions mentioned above could occur at the same time in the core. The neutron yield per alpha particle is a function of initial energy of alpha particle and the composition of the medium in which the alpha particles slow down [10]. The characteristics of the major alpha emitters are listed in Table 2. Those with shorter lifetimes produce alpha particles with higher energy.

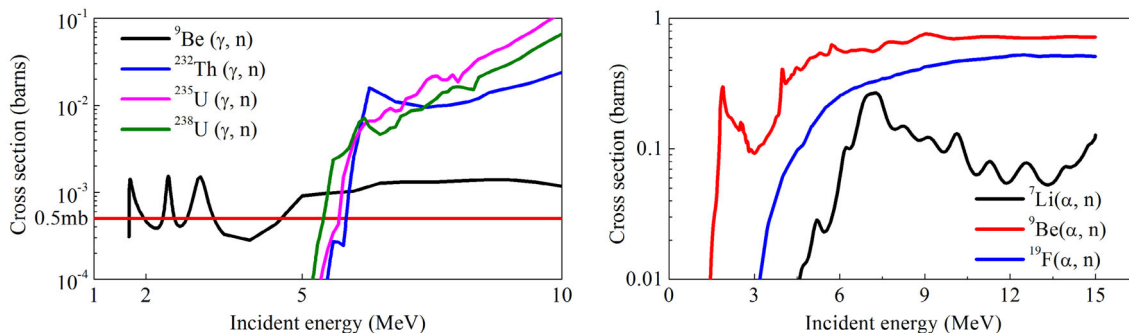


**Fig. 2** (Color online) Cross sections for  $(\gamma, n)$  and  $(\alpha, n)$  reactions

**Table 2** Major alpha emitters and SF neutron emitters

Nuclide	Half-life	Decay mode	Alpha Energy (MeV)	SF neutron		
				Fission prob. per decay	Neutrons per SF	Neutron/s/atom
<sup>242</sup> Cm	163 days	$\alpha$ , SF	6.100	$6.33 \times 10^{-8}$	2.590	$8.07 \times 10^{-15}$
<sup>244</sup> Cm	18.1 a	$\alpha$ , SF	5.805	$1.34 \times 10^{-6}$	2.760	$4.55 \times 10^{-15}$
<sup>240</sup> Pu	6540 a	$\alpha$ , SF	5.256	$3.10 \times 10^{-12}$	2.240	$2.37 \times 10^{-23}$
<sup>239</sup> Pu	$2.41 \times 10^4$ a	$\alpha$ , SF	5.175	$5.70 \times 10^{-8}$	2.160	$1.14 \times 10^{-19}$
<sup>238</sup> U	$4.46 \times 10^9$ a	$\alpha$ , SF	4.270	$5.45 \times 10^{-7}$	2.000	$5.44 \times 10^{-24}$
<sup>235</sup> U	$7.04 \times 10^8$ a	$\alpha$ , SF	4.679	$7.00 \times 10^{-11}$	1.695	$3.76 \times 10^{-27}$

<sup>a</sup>stands for year which is widely used

<sup>o</sup>stands for alpha decay

### 3.1.3 Spontaneous fission neutron

Spontaneous fission (hereafter called SF) is a version of fission that occurs without an inducing neutron being absorbed. Table 2 illustrates that the major decay mode of the SF neutron emitters is alpha decay. Thus, a few SF neutrons are present, and those actinides with shorter lifetime such as <sup>242</sup>Cm and <sup>244</sup>Cm have significantly higher SF neutron yields.

## 3.2 Calculation methods

### 3.2.1 Calculation tools

These calculations were performed with the MCNP6 version 1.0 and SCALE version 6.0. For consistency, the ENDF/B-VII.0 cross-sectional library was used in the calculations.

SCALE (Standardized Computer Analyses for Licensing Evaluation, version 6.0) was developed at ORNL for reactor criticality and safety analyses [17]. In this work, the CSAS6, TRITON, and ORIGEN-S modules in the SCALE program are used. The CSAS6 module is used for criticality calculation. The TRITON module performs the problem-dependent cross-sectional processing followed by a multi-group neutron transport calculation. The ORIGEN-S module is used for depletion and decay calculations.

MCNP is a general purpose Monte Carlo N-Particle code and is very flexible and effective for neutron, photon, or coupled neutron–photon transport. In this work, MCNP6 version 1.0 was used for explicitly representing the core geometry. In the calculations, mode *N* (referred to neutron) *P* (referred to photon) was used. Photonuclear particle production was turned via options on the PHYS: P card—all items were set to the default values except ISPN to  $-1$ , which means analog photonuclear collision sampling.

As the MCNP user manual [18] reminded us, there are only prompt photons (the prompt fission photons ( $\gamma_p$ ) and capture photons ( $\gamma_c$ )) produced in the criticality calculation,

yet the delayed photons ( $\gamma_d$ ) are neglected. Therefore, the intensity and energy spectrum of the delayed photons are calculated by ORIGEN-S module where the photons are calculated based on four different types of process: (1) photons from delayed radioactive decay; (2) photons from ( $\alpha$ , n) reactions; (3) prompt photons from spontaneous fission; and (4) delayed photons from spontaneous fission. The predominant sources of the photons are the decay of fission products and activation products.

Briefly, photoneutrons originating from  $\gamma_p$  and  $\gamma_c$  are computed during the criticality calculation. Meanwhile, photoneutrons due to  $\gamma_d$  are simulated using the general source calculation. With the same model as the criticality calculation, the delayed photons were specified as an isotope volume source by SDEF card that is located in the fuel zone with the energy spectrum calculated by ORIGEN-S module. The photoneutron production rate per source particle was collected from the output file. In print Table 140, there are neutrons/photons nuclide activities of each nuclide in each cell including neutrons produced by photonuclear activities and the average neutron energy. Since the ( $\gamma$ , n) reaction rates are low, the calculations were run for 10 billion source histories. To speed up the process, the energy cutoffs card was used to kill photons with an energy lower than 1.6 MeV during the photon transport.

### 3.2.2 Calculation procedures

Considering the production mechanisms of the inherent neutron sources, we propose a three-step computation process as below.

*First step* Material depletion of different power histories is performed by ORIGEN-S module in SCALE[17], which uses burn-up-dependent cross sections prepared by 3-D Monte Carlo transport calculations [18, 19].

*Second step* The inherent neutron sources from ( $\alpha$ , n) reactions and SF are calculated directly by ORIGEN-S module in SCALE. With the built-in borosilicate glass matrix option, the strength and spectrum of alpha-induced

neutron source are calculated using the constituents in the fuel salt.

**Third step** In theory, the photoneutron production rate could be calculated by integrating the photon flux and the cross section over energy. Subsequently, the total number of photoneutron is calculated by the multiplication of the gamma strength and the reaction rate [2]. In this study, the photoneutron production is calculated using MCNP, which has been widely used for neutron, photon, electron, or coupled neutron/photon/electron transport.

## 4 Results

### 4.1 Photoneutrons

This calculation assumed that the reactor is shut down after continuously operating at full power for 10 days from the beginning. The neutron flux was integrated over the entire energy space, and averaged over spatial space is  $6.8 \times 10^{12}$  n/(cm<sup>2</sup>·s) with the relative standard deviation less than 1%. At zero cooling time, the strength of the prompt photons in the fuel zone—gained after the criticality calculation of MCNP—is  $8.74 \times 10^{17}$  p/s, while the strength of the delayed photons, calculated by ORIGEN-S, is  $6.85 \times 10^{17}$  p/s. The spectra of photons are integrated over the entire space. The spectrum of the prompt photons is harder than the delayed ones. The evolution of the delayed photons after the shutdown is illustrated in Fig. 3. There is a decrease after the shutdown for the delayed photons. The photons with energy greater than 5 MeV decrease sharply, which agrees with the experimental results [20, 21]. This indicates that the high-energy photons are mostly produced by the short-lived emitters. For example, <sup>8</sup>Li and <sup>16</sup>N are the main emitters of 8–10 MeV photons, and their half-lives are 840 ms and 7.13 s, respectively.

The evolutions of the delayed photons after different operation histories are shown in Fig. 4. At zero cooling time (Fig. 4a), the photon spectra remain almost the same

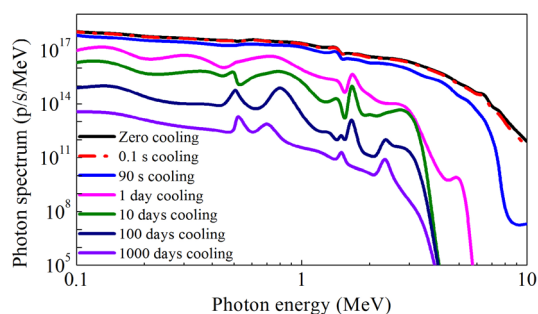


**Fig. 3** (Color online) Delayed photon spectra after shutdown

and are nearly independent of the operation history, which is caused by the large proportion of short-lived gamma in the delayed photons. Upon comparing Fig. 4b–d, it is clear that the delayed photons vary considerably according to the operation history—mainly because of the different unsaturated concentrations of the long-lived gamma emitters such as <sup>142</sup>La, <sup>89</sup>Rb, <sup>138</sup>Cs, <sup>88</sup>Kr. [6]. We deduced that the operation histories mainly affect the photoneutron decrease rate after the shutdown.

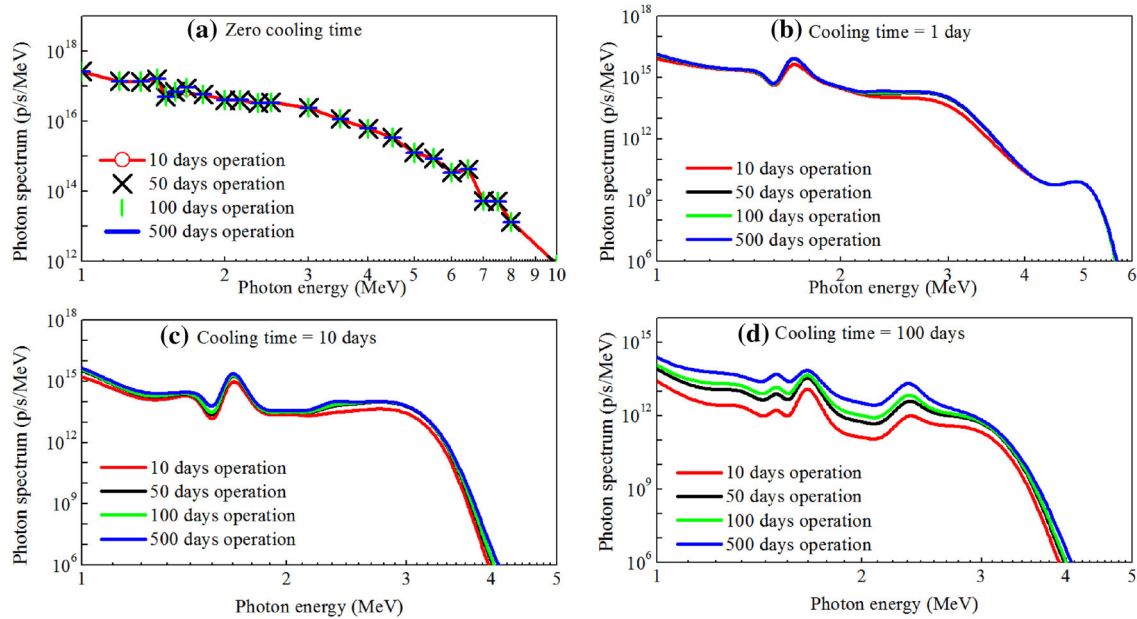
At zero cooling time, the photoneutron fraction in the total neutron population is about  $4.4 \times 10^{-5}$ . This means that the photoneutron forms a negligible part of the neutron population. Figure 5 indicates the relative contributions of the targets and photon emitters to the photoneutron source. The prompt photons account for 87.2% of the photoneutron production, and the delayed photons take up only 12.8%. This confirms the spectrum and strength differences. For the targets, the <sup>9</sup>Be is rated first at 53.9% followed by <sup>238</sup>U at 38.0% and <sup>235</sup>U at 7.2%. The remaining parts are less than 1% and are produced by other targets such as <sup>236</sup>U, <sup>239</sup>Pu, <sup>232</sup>Th, etc.

Table 3 presents the photoneutron yield, delayed photon source, and photoneutron source at selected cooling time. The photoneutron source reduces dramatically due to degrade of photon source after the shutdown. There is a slight fluctuation in the decline process of photoneutron yield after shutdown, which may be caused by fluctuations of the <sup>9</sup>Be ( $\gamma, n$ ) cross sections. The calculation indicates that the <sup>9</sup>Be ( $\gamma, n$ ) reaction takes up 98% of photoneutron production with delayed photons in the core only at zero cooling time; the average energy of the photoneutrons is 0.45 MeV.

### 4.2 Alpha-induced neutron

The strength of alpha-induced neutron source and their average energies are listed in Table 4. We assumed that the power level is constantly 2 MW in operation, and the cooling time is zero. At zero operation time, the main alpha emitter is <sup>238</sup>U. It produces 4.270 MeV alpha particles that account for 99.99% alpha production in the core. After operation for 10 days, the high-energy alpha emitter <sup>240</sup>Pu is accumulated in the burn-up process. It produces 5.256 MeV alpha particles that account for 0.09% production in the core. The cross section of <sup>7</sup>Li ( $\alpha, n$ ) at 4.42 MeV is 0.0066 barns, and it increases to 0.0285 barns at 5.2 MeV. That explains the proportion jump of alpha particles produced by <sup>7</sup>Li after 10 days of operation.

When the operation time increased from 0 to 500 days, the strength of alpha source rose gradually from  $4.56 \times 10^9$  to  $6.36 \times 10^{11}$   $\alpha$ /s, and the average energy increases slightly from 4.469 to 5.105 MeV. The strength of the alpha-induced neutron source rises accordingly, but



**Fig. 4** (Color online) Photon spectra evolution after shutdown for different operation times

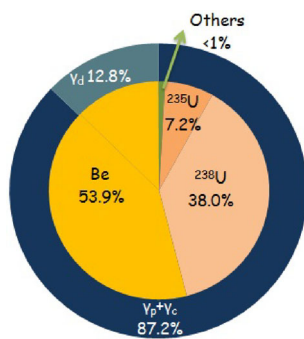


**Fig. 5** (Color online) Photoneutron pie chart

the average energy showed a clear opposite trend that may be caused by the proportion changes in the targets. The  ${}^7\text{Li}$  targets produce a slight amount of neutrons due to higher threshold and lower  $(\alpha, n)$  cross section than  ${}^{19}\text{F}$  and  ${}^9\text{Be}$  targets as shown in Sect. 3. In general, the increase in the energy of alpha particles favors  ${}^{19}\text{F}(\alpha, n)$  and  ${}^7\text{Li}(\alpha,$

$n)$  reactions more, and these may be caused by the fluctuations in  ${}^9\text{Be}(\alpha, n)$  cross section. Although  ${}^9\text{Be}$  has higher cross section and lower threshold,  ${}^{19}\text{F}$  takes a larger part in the fuel and this makes them almost equally important after power operation. Alpha particles are mainly emitted by the long-lived nuclides like  ${}^{239,240}\text{Pu}$  rather than the short-lived nuclides like  ${}^{242}\text{Cm}$  as in commercial reactors; this is because it is low burn-up fuel [2].

### 4.3 Spontaneous fission neutron

Table 4 shows that the SF neutron source increases gradually, and the average energy rises slowly. The major contributors are listed in Table 4, and the long-lived emitters take more shares due to the low burn-up. Compared to the alpha-induced neutron source, the SF neutron source is remarkably weaker especially after long-term operation. Alpha-induced neutrons are about eightfold as strong as SF neutrons in the fresh core, and this ratio

**Table 3** Photoneutron source after shutdown

Cooling time	Delayed photon source (p/s)	Photoneutron yield ( $n/10^6$ p)	Photoneutron source (n/s)
0 s	$6.854 \times 10^{17}$	1.249	$8.561 \times 10^{11}$
0.1 s	$6.810 \times 10^{17}$	1.238	$8.431 \times 10^{11}$
90 s	$4.013 \times 10^{17}$	0.813	$3.263 \times 10^{11}$
1 day	$6.337 \times 10^{16}$	0.080	$5.101 \times 10^9$
10 days	$1.088 \times 10^{16}$	0.228	$2.481 \times 10^9$
100 days	$7.248 \times 10^{14}$	0.024	$1.740 \times 10^7$
1000 days	$1.591 \times 10^{13}$	0.030	$4.773 \times 10^5$
10000 days	$2.513 \times 10^{12}$	0.001	$2.513 \times 10^3$

**Table 4** SF neutron source and alpha-induced neutron source

Operation time (days)	SF neutron source				Alpha-induced neutron source				
	Strength (n/s)	Energy (MeV)	Contributions (%)		Strength (n/s)	Energy (MeV)	Contributions (%)		
			<sup>240</sup> Pu	<sup>238</sup> U			<sup>19</sup> F	<sup>9</sup> Be	<sup>7</sup> Li
0	$2.31 \times 10^3$	1.688	0.00	99.99	$1.81 \times 10^4$	3.289	37.58	62.39	0.02
10	$2.32 \times 10^3$	1.688	0.09	99.89	$1.00 \times 10^5$	2.985	47.89	50.04	2.07
50	$2.39 \times 10^3$	1.696	3.32	96.65	$5.87 \times 10^5$	2.929	49.78	47.48	2.44
100	$2.65 \times 10^3$	1.719	12.61	87.33	$1.20 \times 10^6$	2.923	49.97	47.55	2.48
200	$3.69 \times 10^3$	1.780	36.91	62.65	$2.45 \times 10^6$	2.920	50.08	47.42	2.50
500	$1.16 \times 10^4$	1.900	70.57	19.91	$6.45 \times 10^6$	2.918	50.30	47.12	2.59

exceeds 500-fold after power operation for 500 days. The reason is that most SF emitters have much higher alpha decay rate than SF rate such as <sup>242</sup>Cm, <sup>240</sup>Pu, <sup>239</sup>Pu.

**4.4 Analysis on canceling the secondary source**

The neutron source evolution following shutdown after 10 days full power operation is shown in Fig. 6 (left). The curve can be divided into three regions: (1) the delayed neutron hold-up region; (2) the photoneutron hold-up region; and (3) the alpha-induced neutron hold-up region. After shutdown, the delayed neutron source declines quickly, and the photoneutron becomes dominant about two minutes later. Eventually, the alpha-induced neutron source becomes greater than the photoneutron source. The alpha-induced neutron source and SF neutron source remain nearly constant in the time zone of interest. One unique feature of MSR is that the liquid fuel salt is flowing through the core and the whole primary circuit. It simultaneously acts like the fuel and the coolant. Hence, the delayed neutron precursors are circulated with the fuel salt, which causes precursor loss in the circuit; the delayed neutron source in Fig. 6 is overestimated.

The inherent neutron source evolutions after operation at 2 MW for periods of 10, 50, 100, and 500 days are exhibited in Fig. 6 (right). This focuses on regions 2 and 3 as previously defined. This shows that the longer operation time slows down the decrease, which confirms the variation trend of the photon sources shown in Fig. 4. Referring to the national standard [22] “Criteria for nuclear reactor instrumentation Part 1: General principles,” the count rate of 2 cps or more should be maintained whenever the fuel is in the core. When the  $k_{eff}$  is about 0.99, the count rates should be greater than 10 cps; when the installed neutron source is used and  $k_{eff}$  is about 0.99, at least 95% of the measured neutrons should be produced by fission. The estimated installed neutron source is  $4 \times 10^7$  n/s and is located in the central channel [16]. Unlike the installed source, the inherent neutron sources are homogeneously distributed in the fuel salt that may be more beneficial for the measurement under subcritical conditions. As long as the inherent neutrons are stronger than the estimated neutron source, the surveillance would be highly reliable without an installed source. Figure 6 shows that if the reactor had been continuously operated at full power for 10 days, then the inherent neutrons would be sufficiently

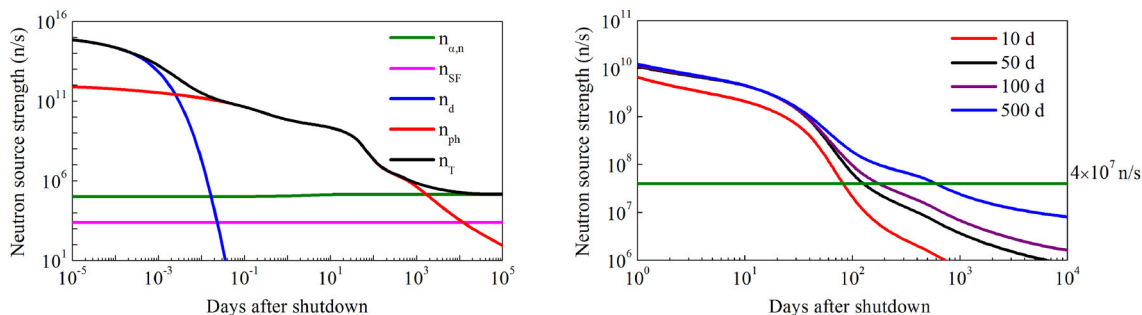


**Fig. 6** (Color online) Neutron sources for different cooling times (left) and operation histories (right). ( $n_{\alpha, n}$ : alpha-induced neutrons;  $n_{SF}$ : SF neutrons;  $n_d$ : delayed fission neutrons;  $n_{ph}$ : photoneutrons;  $n_T$ : all neutrons)

strong within 80 days after the shutdown. If operated for 500 days, then the installed neutrons would be no longer needed within 2 years after the shutdown.

## 5 Conclusion

Due to a large quantity of beryllium in the fuel salt and the mixing of actinides with light nucleus, the inherent neutron sources in the MSR are much stronger than the traditional reactors that use solid fuel and do not have a large amount of beryllium or deuterium in the core. Here, the inherent neutron sources including photoneutrons, alpha-induced neutrons, and SF neutrons are calculated at selected operation and cooling time using SCALE and MCNP based on a simple full core MSR model. Conclusions drawn from this study are as follows:

- (1) In the fresh core, the inherent neutron sources are as strong as  $2.04 \times 10^4$  n/s in which alpha-induced neutron sources account for 89%, and SF neutrons take up 11%. However, they are not sufficiently strong to eliminate the installed source.
- (2) After power operation, the inherent neutron sources are much stronger due to photoneutrons. During power operation, the inherent neutron sources form an insignificant part of the total neutron population, and beryllium targets account for about 54% production of the photoneutrons.
- (3) After the shutdown, the surveillance would be highly reliable without the installed neutron source as long as the inherent neutron sources are sufficiently strong. After 10 days of continuous power operation, there would be no need for the installed source within 80 days after shutdown. Similarly, the installed source could be eliminated within 2 years after 500 days of continuous operation.

Here, we report results of SF neutrons and alpha-induced neutrons that were directly obtained from the deterministic code ORIGEN-S. In other words, the uncertainties of these results come from the neutron transport calculation that produces problem-dependent neutron spectrum. In this work, the relative standard deviation of neutron flux integrated over the entire phase space is less than 1%. Thus, 1% relative standard deviation of the results (SF neutron and alpha-induced neutron) is expected. The results of photoneutrons are calculated by MCNP code using continuous cross sections. The uncertainties of the photoneutrons mainly come from the photon flux. The relative standard deviation of photon flux integrated over whole phase space is less than 1% in the calculation. Therefore, the relative standard deviation of the

photoneutron results is less than 1%. The uncertainties from nuclear data will be analyzed in the near future.

## References

1. Y.Q. Shi, *Experimental methods in the nuclear reactor*, 1st edn. (Atomic Energy Press, Beijing, 2011), pp. 46–64 (in Chinese)
2. M. Watanabe, A. Yamamoto, Y. Yamane, Measuring the photoneutron originating from  $D(\gamma, n)H$  reaction after the shutdown of an operational BWR. *J. Nucl. Sci. Technol.* **46**, 1099–1112 (2009). <https://doi.org/10.1080/18811248.2009.9711622>
3. F. Jatuff, A. Lüthi, M. Murphy et al., Measurement and interpretation of delayed photoneutrons effects in multizone criticals with partial  $D_2O$  moderation. *Ann. Nucl. Energy* **30**, 1731–1755 (2003). [https://doi.org/10.1016/S0306-4549\(03\)00136-1](https://doi.org/10.1016/S0306-4549(03)00136-1)
4. S. Li., L. Deng, H. B. Xu, et al., Usability analyses of source range detector after secondary neutron source canceled. *At. Energy Sci. Technol.* **45**, 314–318 (2011) (in Chinese)
5. L.J. Fei., R. Le, Analyses on cancelling secondary neutron source in Changjiang NPP. *Plant Maintenance Eng.* **z1**, 13–16 (2015). <https://doi.org/10.3969/j.issn.1001-0599.2015.z1.005> (in Chinese)
6. M.S. Onegin, Delayed photoneutrons in the PIK reactor. *At. Energy* **107**, 194–201 (2009). <https://doi.org/10.1007/s10512-010-9215-1>
7. I. Khamis, Evaluation of the photo-neutron source in the syrian miniature neutron source reactor. *Ann. Nucl. Energy* **29**, 1365–1371 (2002). [https://doi.org/10.1016/S0306-4549\(01\)00114-1](https://doi.org/10.1016/S0306-4549(01)00114-1)
8. S. Birikorang, E. Akaho, B. Nyarko et al., Feasibility study of photo-neutron flux in various irradiation channels of Ghana MNSR using a Monte Carlo code. *Ann. Nucl. Energy* **38**, 1593–1597 (2011). <https://doi.org/10.1016/j.anucene.2011.03.004>
9. P.N. Haubenreich, J.R. Engel, B.E. Prince, et al., MSRE design and operations report Part III. Nuclear analysis. ORNL, ORNL-TM-0730, USA (1969)
10. P.N. Haubenreich, Inherent neutron sources in clean MSRE fuel salt. ORNL, ORNL-TM-0611, USA (1963)
11. R.C. Steffy, Jr., Inherent neutron sources in MSRE with clean  $^{233}U$  fuel. ORNL, ORNL-TM-2685, USA (1969)
12. J.R. Engel, P.N. Haubenreich, B.E. Prince., MSRE neutron source requirements. ORNL, ORNL-TM-0935, USA (1964)
13. W.N. Powell., Reconsideration of inherent neutron sources in liquid fuel of molten salt reactors. Master's thesis, The Ohio State University, 2013
14. W. Wilson, R. Perry, W. Charlton et al., Sources: a code for calculating (alpha, n), spontaneous fission, and delayed neutron sources and spectra. *Prog. Nucl. Energy* **51**, 608–613 (2009). <https://doi.org/10.1016/j.pnucene.2008.11.007>
15. Z Dai, W Liu, Thorium-based Molten Salt Reactor (TMSR) project in China. Proceedings of the conference on molten salts in nuclear technology, Mumbai, India, 9–11 Feb 2013
16. TMSR group, Pre-conceptual design of the 2 MW liquid fueled molten salt reactor and pyroprocess demonstration facility (2014)
17. SCALE: A Comprehensive Modeling and Simulation Suite for Nuclear Safety Analysis and Design. ORNL, ORNL/TM-2005/39, USA (2011)
18. D.B. Pelowitz (ed.), MCNP6<sup>TM</sup> User's Manual, Los Alamos National Laboratory, LA-CP-13-00634, USA (2013)



19. D.P. Heinrichs, E.M. Lent., Photonuclear benchmarks with a comparison of COG and MCNPX results. Brookhaven National Laboratory, UCRL-CONF-200552, USA (2003)
20. H. Kröhnert, G. Perreta, M.F. Murphy et al., Freshly induced short-lived gamma-ray activity as a measure of fission rates in lightly re-irradiated spent fuel. Nucl. Instrum. Methods Phys. Res. Sect. A **624**, 101–108 (2010). <https://doi.org/10.1016/j.nima.2010.09.033>
21. M. Švadlenková, L. Heraltováb, V. Juriček et al., Gamma spectrometry of short living fission products in fuel pins. Nucl. Instrum. Methods Phys. Res. Sect. A **739**, 55–62 (2014). <https://doi.org/10.1016/j.nima.2013.12.019>
22. G. 12789.1, Criteria for nuclear reactor instrumentation Part 1: General principles, 1991